

Approximations of MINFLUX Localization Precision with Background

Zach Marin^{1,2}, Jonas Ries^{1,2,3,4}

¹Max Perutz Labs, Vienna Biocenter Campus (VBC), Vienna, Austria

²University of Vienna, Center for Molecular Biology, Department of Structural and Computational Biology, Vienna, Austria

³European Molecular Biology Laboratory, Cell Biology and Biophysics, Heidelberg, Germany

⁴University of Vienna, Faculty of Physics, Vienna, Austria

Correspondence: jonas.ries@univie.ac.at

Abstract

MINFLUX [1] is an emerging super-resolution technology that measures the position of single fluorophores with nanometer precision using fewer photons than any other fluorescence imaging or tracking technique. Here, we derive simple and instructive analytical equations for MINFLUX localization precision with a special focus on background photons. A fluorescence background, either arising from an imperfect zero of the MINFLUX excitation point spread function (PSF) or from auto- or out-of-focus fluorescence, ultimately limits the resolution achievable with MINFLUX. Building on previous work [1–3], we try to improve our understanding of the influence of background, especially when it is unknown, through a new set of expressions for the localization precision, based on an explicit background term instead of signal-to-background ratio. We use these equations to generate an intuitive understanding of how fluorescence background affects MINFLUX measurements and illustrate that:

- The precision of an emitter position estimate depends on the gradient of its excitation profile.
- Knowledge of the fluorescence background, obtained during post-processing of MINFLUX traces or through separate measurements, provides a better localization precision than in the case of unknown background.
- In diffraction-limited systems, localization with a PSF that features a near-zero minimum outperforms localization with a maximum.

We also present an analytical expression for the localization precision in orbital tracking [4], which we use for comparison to MINFLUX. Non-trivial derivations presented in this paper can be found in the accompanying Mathematica notebook.

1 Deriving the Cramér-Rao bound for K measurements of an emitter in the presence of background in 1D

There is an emitter sitting on a line. We want to know its position x_0 , so we probe it with an excitation PSF of shape $f(x)$ positioned at x_i . We assume the pinhole is large, so we always collect all of the emission signal. The intensity measured from an emitter positioned at x_0 can be expressed as

$$I(x_0 - x_i) = I_0(f(x_0 - x_i) + b), \quad (1)$$

where $I(x_0 - x_i)$ is the collected intensity, i.e. the number of detected photons, n_i , I_0 is a proportionality factor that describes how the brightness of the emitter depends on the illumination laser power, and b is the proportion of signal arising from the background. It is instructive to express b as multiplied by I_0 since the background, which arises from auto- or out-of-focus fluorescence background or, in case of probing with a local minimum, from an imperfect zero in the PSF, will scale with illumination laser power.

Let us investigate the precision with which we can localize a fluorophore from a single measurement, provided we know the brightness of the fluorophore I_0 . For simplicity, we place the PSF at $x_i = 0$ and neglect background

($b = 0$). Then, the number of photons we detect is $N = I_0 f(x_0)$. We can determine the fluorophore position as $x_0 = f^{-1}(N/I_0)$. In a linear approximation, the error of the position δx_0 is proportional to the error δN in measuring the photons N :

$$\delta N = \frac{\partial I}{\partial x_0} \delta x_0 = I_0 f'(x_0) \delta x_0, \quad (2)$$

where $f'(x_0) = \partial f / \partial x|_{x_0}$ is the derivative of f along x , i.e., the gradient of the excitation PSF, evaluated at x_0 .

Because the detection of photons is a Poisson process, $\delta N = \sqrt{N}$. We can substitute $I_0 = N/f(x_0)$ and solve for δx_0 :

$$\delta x_0 = \left| \frac{1}{\sqrt{N}} \frac{f(x_0)}{f'(x_0)} \right|, \quad (3)$$

where we have taken the absolute value since localization precision is always positive. Thus, in a first approximation, the position error scales inversely with \sqrt{N} and is proportional to the ratio of magnitude $f(x_0)$ and gradient $f'(x_0)$ of the excitation PSF at the position of the emitter. For realistic measurements, the fluorophore brightness is typically not known, and we need to perform additional measurements.

To examine the localization precision in the case when we make sufficient measurements to capture fluorophore brightness, position, and background, we derive the localization precision using Fisher information and the Cramér-Rao (lower) bound (CRB).

The Fisher information is usually expressed as a matrix where each element is calculated as

$$\mathcal{I}_{l,m}(x_0) = \sum_{i=1}^K \frac{1}{I(x_0 - x_i)} \frac{\partial I(x_0 - x_i)}{\partial \theta_l} \frac{\partial I(x_0 - x_i)}{\partial \theta_m}, \quad (4)$$

where $\theta \in \{I_0, x_0, b\}$. We call the number of unknown variables M , which in this case is 3. In this paper, we slightly modify Eq. 4 by following the framework outlined in Masullo et al. [3]. We assume pure Poisson noise and call N the total number of photons detected over K exposures with the excitation PSF at positions x_i . The probability of collecting n_i photons during one of these measurements $i \in K$ is

$$p_i(x_0) = \frac{I(x_0 - x_i)}{\sum_{j=1}^K I(x_0 - x_j)}. \quad (5)$$

We can now compute the elements of the Fisher information matrix as

$$\mathcal{I}_{l,m}(x_0) = N \sum_{i=1}^K \frac{1}{p_i(x_0)} \frac{\partial p_i(x_0)}{\partial \theta_l} \frac{\partial p_i(x_0)}{\partial \theta_m}, \quad (6)$$

where we have made the substitution $I(x_0 - x_i) = N p_i(x_0)$ where $N = \sum_{i=1}^K n_i$. This substitution eliminates I_0 from the Fisher information matrix (and wraps it in N), allowing us to compute the matrix for M unknowns using $M - 1$ variables [2], $\theta \in \{x_0, b\}$. Even with this substitution, we still require $K \geq M$ exposures to compute M unknown variables.

1.1 In the case of known background

Suppose we have previously measured the background offset b in our experiment, or we can extract it from our measurements in a post-processing analysis. In this case, $I(x_0 - x_i)$ as expressed in Eq. 1 has only two unknowns: I_0 and x_0 . To estimate these unknowns from the measured number of photons n_i , K must be ≥ 2 . The Fisher information matrix in this case is a single entry,

$$\mathcal{I}(x_0) = N \sum_{i=1}^K \frac{1}{p_i} \left(\frac{\partial p_i}{\partial x_0} \right)^2, \quad (7)$$

where $N = \sum_{i=1}^K n_i$ is the total number of photons detected over K exposures and p_i is as defined in Eq. 5.

The theoretically best achievable localization precision can be estimated as the square root of the CRB, Σ_{CRB} , which is the inverse of the Fisher information matrix, $\mathcal{I}(x_0)$. The localization precision in the case of known background for $K = 2$ is then

$$\sigma_{x_0} = \sigma_{\text{CRB}} = \sqrt{\Sigma_{\text{CRB}}} = \sqrt{\mathcal{I}(x_0)^{-1}} = \sqrt{\frac{1}{N \left(\frac{1}{p_1} \left(\frac{\partial p_1}{\partial x_0} \right)^2 + \frac{1}{p_2} \left(\frac{\partial p_2}{\partial x_0} \right)^2 \right)}}, \quad (8)$$

and for $K = 3$ it is

$$\sigma_{x_0} = \sqrt{\frac{1}{N \left(\frac{1}{p_1} \left(\frac{\partial p_1}{\partial x_0} \right)^2 + \frac{1}{p_2} \left(\frac{\partial p_2}{\partial x_0} \right)^2 + \frac{1}{p_3} \left(\frac{\partial p_3}{\partial x_0} \right)^2 \right)}}. \quad (9)$$

1.1.1 Equivalence with signal-to-background ratio formulation

In [1–3], and other places, the derivation for MINFLUX localization precision expresses the intensity response of an emitter as

$$I_{\text{nobg}}(x_0 - x_i) = I_0 f(x_0 - x_i), \quad (10)$$

where I_0 , $f(x)$, x_i , and x_0 are as in Eq. 1. The background is included as a signal-to-background ratio

$$\text{SBR}(x_0) = \frac{\sum_{j=1}^K I_{\text{nobg}}(x_0 - x_j)}{\sum_{j=1}^K b_j}, \quad (11)$$

in $p_i(x_0)$, rather than in $I(x_0 - x_i)$. By setting $b_j = b_0 \forall j$, it is possible to express $p_i(x_0)$ as

$$p_i(x_0) = \frac{\text{SBR}(x_0)}{\text{SBR}(x_0) + 1} \frac{I_{\text{nobg}}(x_0 - x_i)}{\sum_{j=1}^K I_{\text{nobg}}(x_0 - x_j)} + \frac{1}{\text{SBR}(x_0) + 1} \frac{1}{K}. \quad (12)$$

We can recover $p_i(x_0)$ in the form of Eq. 5 by substituting the definition of SBR back in to Eq. 12 and using the trivial substitution $b_0 = I_0 b$, where I_0 is as defined in Eq. 10. Then,

$$p_i(x_0) = \frac{\frac{\sum_{j=1}^K I_{\text{nobg}}(x_0 - x_j)}{K I_0 b}}{\frac{\sum_{j=1}^K I_{\text{nobg}}(x_0 - x_j)}{K I_0 b} + 1} \frac{I_{\text{nobg}}(x_0 - x_i)}{\sum_{j=1}^K I_{\text{nobg}}(x_0 - x_j)} + \frac{1}{\frac{\sum_{j=1}^K I_{\text{nobg}}(x_0 - x_j)}{K I_0 b} + 1} \frac{1}{K} \quad (13)$$

$$= \frac{1}{\frac{\sum_{j=1}^K I_{\text{nobg}}(x_0 - x_j)}{K I_0 b} + 1} \left(\frac{I_{\text{nobg}}(x_0 - x_i)}{K I_0 b} + \frac{1}{K} \right) \quad (14)$$

$$= \frac{1}{\frac{\sum_{j=1}^K I_{\text{nobg}}(x_0 - x_j)}{K I_0 b} + \frac{K I_0 b}{K I_0 b}} \left(\frac{I_{\text{nobg}}(x_0 - x_i)}{K I_0 b} + \frac{I_0 b}{K I_0 b} \right) \quad (15)$$

$$= \frac{I_{\text{nobg}}(x_0 - x_i) + I_0 b}{\sum_{j=1}^K I_{\text{nobg}}(x_0 - x_j) + I_0 b}, \quad (16)$$

which is equivalent to Eq. 5. In [1–3], the derivative of the SBR is not considered in the Fisher information matrix. Thus, the SBR formulation and the known background formulation are equivalent.

1.2 In the case of unknown background

Suppose we have not previously measured our background offset. We want to understand how background influences our emitter localization precision, so we now include it in $\mathcal{I}(x_0)$:

$$\mathcal{I}(x_0) = N \sum_{i=1}^K \frac{1}{p_i} \begin{bmatrix} \left(\frac{\partial p_i}{\partial x_0} \right)^2 & \frac{\partial p_i}{\partial x_0} \frac{\partial p_i}{\partial b} \\ \frac{\partial p_i}{\partial b} \frac{\partial p_i}{\partial x_0} & \left(\frac{\partial p_i}{\partial b} \right)^2 \end{bmatrix}. \quad (17)$$

In this case, $I(x_0 - x_i)$ as defined in Eq. 1 has three unknowns: I_0 , x_0 , and b . To estimate these unknowns from the measured number of photons n_i , K must be ≥ 3 . For $K = 3$,

$$\mathcal{I}(x_0) = N \begin{bmatrix} \frac{1}{p_1} \left(\frac{\partial p_1}{\partial x_0} \right)^2 + \frac{1}{p_2} \left(\frac{\partial p_2}{\partial x_0} \right)^2 + \frac{1}{p_3} \left(\frac{\partial p_3}{\partial x_0} \right)^2 & \frac{1}{p_1} \left(\frac{\partial p_1}{\partial x_0} \frac{\partial p_1}{\partial b} \right) + \frac{1}{p_2} \left(\frac{\partial p_2}{\partial x_0} \frac{\partial p_2}{\partial b} \right) + \frac{1}{p_3} \left(\frac{\partial p_3}{\partial x_0} \frac{\partial p_3}{\partial b} \right) \\ \frac{1}{p_1} \left(\frac{\partial p_1}{\partial b} \frac{\partial p_1}{\partial x_0} \right) + \frac{1}{p_2} \left(\frac{\partial p_2}{\partial b} \frac{\partial p_2}{\partial x_0} \right) + \frac{1}{p_3} \left(\frac{\partial p_3}{\partial b} \frac{\partial p_3}{\partial x_0} \right) & \frac{1}{p_1} \left(\frac{\partial p_1}{\partial b} \right)^2 + \frac{1}{p_2} \left(\frac{\partial p_2}{\partial b} \right)^2 + \frac{1}{p_3} \left(\frac{\partial p_3}{\partial b} \right)^2 \end{bmatrix} \quad (18)$$

and Σ_{CRB} is

$$\Sigma_{\text{CRB}} = \frac{1}{cN} \begin{bmatrix} \frac{1}{p_1} \left(\frac{\partial p_1}{\partial b} \right)^2 + \frac{1}{p_2} \left(\frac{\partial p_2}{\partial b} \right)^2 + \frac{1}{p_3} \left(\frac{\partial p_3}{\partial b} \right)^2 & -\frac{1}{p_1} \left(\frac{\partial p_1}{\partial x_0} \frac{\partial p_1}{\partial b} \right) - \frac{1}{p_2} \left(\frac{\partial p_2}{\partial x_0} \frac{\partial p_2}{\partial b} \right) - \frac{1}{p_3} \left(\frac{\partial p_3}{\partial x_0} \frac{\partial p_3}{\partial b} \right) \\ -\frac{1}{p_1} \left(\frac{\partial p_1}{\partial b} \frac{\partial p_1}{\partial x_0} \right) - \frac{1}{p_2} \left(\frac{\partial p_2}{\partial b} \frac{\partial p_2}{\partial x_0} \right) - \frac{1}{p_3} \left(\frac{\partial p_3}{\partial b} \frac{\partial p_3}{\partial x_0} \right) & \frac{1}{p_1} \left(\frac{\partial p_1}{\partial x_0} \right)^2 + \frac{1}{p_2} \left(\frac{\partial p_2}{\partial x_0} \right)^2 + \frac{1}{p_3} \left(\frac{\partial p_3}{\partial x_0} \right)^2 \end{bmatrix} \quad (19)$$

where

$$c = \left(\frac{1}{p_2 p_3} \left(\frac{\partial p_3}{\partial x_0} \frac{\partial p_2}{\partial b} - \frac{\partial p_2}{\partial x_0} \frac{\partial p_3}{\partial b} \right)^2 + \frac{1}{p_1} \left(\frac{1}{p_2} \left(\frac{\partial p_2}{\partial x_0} \frac{\partial p_1}{\partial b} - \frac{\partial p_1}{\partial x_0} \frac{\partial p_2}{\partial b} \right)^2 + \frac{1}{p_3} \left(\frac{\partial p_3}{\partial x_0} \frac{\partial p_1}{\partial b} - \frac{\partial p_1}{\partial x_0} \frac{\partial p_3}{\partial b} \right)^2 \right) \right). \quad (20)$$

The localization precision σ_{x_0} is given by the standard deviation $\sigma_{\text{CRB},i,j} = \sqrt{\Sigma_{\text{CRB},i,j}}$ for the upper left element,

$$\sigma_{x_0} = \sigma_{\text{CRB},1,1} = \sqrt{\frac{\frac{1}{p_1} \left(\frac{\partial p_1}{\partial b} \right)^2 + \frac{1}{p_2} \left(\frac{\partial p_2}{\partial b} \right)^2 + \frac{1}{p_3} \left(\frac{\partial p_3}{\partial b} \right)^2}{N \left(\frac{1}{p_2 p_3} \left(\frac{\partial p_3}{\partial x_0} \frac{\partial p_2}{\partial b} - \frac{\partial p_2}{\partial x_0} \frac{\partial p_3}{\partial b} \right)^2 + \frac{1}{p_1} \left(\frac{1}{p_2} \left(\frac{\partial p_2}{\partial x_0} \frac{\partial p_1}{\partial b} - \frac{\partial p_1}{\partial x_0} \frac{\partial p_2}{\partial b} \right)^2 + \frac{1}{p_3} \left(\frac{\partial p_3}{\partial x_0} \frac{\partial p_1}{\partial b} - \frac{\partial p_1}{\partial x_0} \frac{\partial p_3}{\partial b} \right)^2 \right) \right)}. \quad (21)$$

We can see that, as in the simpler cases, the accuracy of the emitter position estimate is dependent on the derivatives of $p_i(x_0)$, and thus dependent on the derivatives of $I(x_0 - x_i)$ with respect to x_0 , $\partial I(x_0 - x_i)/\partial x_0$, which is proportional to the excitation PSF gradient at the emitter position.

2 Localization precision of emitters in 1D

Now armed with analytical expressions, we can explicitly compute the localization precision of emitters in 1D for specific PSFs.

2.1 Minimum

The quadratic equation is a good approximation of the center of the donut PSF commonly used in MINFLUX [1]. We define a 1D quadratic PSF with background as

$$I_{\text{quad},1\text{D}}(x_0 - x_i) = I_0 \left(\frac{(x_0 - x_i)^2}{2\sigma_q^2} + b \right), \quad (22)$$

where I_0 , x_i , x_0 , and b are as defined in Eq. 1 and σ_q parameterizes the steepness of the PSF. It is important to note that σ_q cannot be smaller than what is allowed by the diffraction limit of the system optics (~ 250 nm).

For $b = 0$, the localization precision of the simple single-point measurement (Eq. 3) is

$$\delta x_0 = \frac{x_0}{2\sqrt{N}}. \quad (23)$$

2.1.1 Minimum with known background

Suppose we know the background, e.g. through measurement of the average response $I_{\text{quad},1\text{D}}(x_0 - x_i)$ in empty space. In this case, we can substitute Eq. 22 evaluated at $x_i = -L/2$, and $L/2$, where $L \in \mathcal{R}$ describes the displacement between the two measurements, into Eqs. 5 and 8 to get

$$\sigma_{x_0} = \frac{1}{4L\sqrt{N}} \sqrt{\frac{(8b\sigma_q^2 + L^2 + 4x_0^2)^2 \left(16b\sigma_q^2 (4b\sigma_q^2 + L^2 + 4x_0^2) + (L^2 - 4x_0^2)^2 \right)}{(8b\sigma_q^2 + L^2 - 4x_0^2)^2}}. \quad (24)$$

For $b = 0$, this simplifies to

$$\sigma_{x_0}(b = 0) = \frac{L}{4\sqrt{N}} \left[1 + \left(\frac{x_0}{L/2} \right)^2 \right], \quad (25)$$

which is equivalent to the corresponding Eq. S22b found in the supplement of [1]. If we further let $x_0 = 0$, we get

$$\sigma_{x_0}(x_0 = 0, b = 0) = \frac{L}{4\sqrt{N}}. \quad (26)$$

Note that the single-measurement approximation Eq. 23 measured at $x_0 = L/2$ is equivalent to Eq. 26.

In the case Eq. 22 is evaluated at three points, $x = -L/2, 0$, and $L/2$, and substituted into into Eqs. 5 and 9, we get

$$\sigma_{x_0} = \frac{1}{4L\sqrt{N}} \sqrt{\frac{2(2b\sigma_q^2 + x_0^2)(12b\sigma_q^2 + L^2 + 6x_0^2)^2 \left(16b\sigma_q^2(4b\sigma_q^2 + L^2 + 4x_0^2) + (L^2 - 4x_0^2)^2 \right)}{\left(4b\sigma_q^2(4b\sigma_q^2(24b\sigma_q^2 + 5L^2 - 12x_0^2) + L^4 + 6L^2x_0^2 - 24x_0^4) + 3x_0^2(L^2 - 4x_0^2)^2 \right)}}. \quad (27)$$

At $x_0 = 0$, Eq. 27 simplifies to

$$\sigma_{x_0}(x_0 = 0) = \frac{1}{4L\sqrt{N}} \sqrt{(L^2 + 8b\sigma_q^2)(L^2 + 12b\sigma^2)}, \quad (28)$$

and in the case of no background ($b = 0$), Eq. 28 simplifies to

$$\sigma_{x_0}(x_0 = 0, b = 0) = \frac{L}{4\sqrt{N}}, \quad (29)$$

which is equivalent to the value of the two-point case at the same position and background (Eq. 26).

2.1.2 Minimum with an unknown background

Suppose we have not measured our background signal and we measure at three points, $x_i = -L/2, 0$, and $L/2$. We plug $I_{\text{quad,1D}}(x_0 - x_i)$ into equations 5 and 21 to get

$$\sigma_{x_0} = \frac{1}{4L^2\sqrt{N}} \sqrt{(12b\sigma_q^2 + L^2 + 6x_0^2) \left(8b(L^2 + 48x_0^2)\sigma_q^2 + L^4 - 12L^2x_0^2 + 192x_0^4 \right)}. \quad (30)$$

At $x_0 = 0$, Eq. 30 simplifies to 28, suggesting that the known and unknown background cases are equivalent. However, away from $x_0 = 0$, the localization precision in the cases of assumed unknown (Eq. 30) and assumed known (Eq. 27) background differ significantly, as shown in Figure 1. Knowing the background (i.e. having more information) results in a better localization precision.

For the example shown in Figure 1 where the background value is known, it is possible to convert directly between b and SBR via substitution:

$$\begin{aligned} \text{SBR}(x_0 = 0) &= \frac{\sum_{j=1}^K I(x_j)}{Kb} \\ &= \frac{I(-50/2) + I(0) + I(50/2)}{(3)(0.01)} \\ &\approx 1.33. \end{aligned}$$

2.1.3 Localization precision in the presence of different background sources

The fluorescence background b (Eq. 1) in a MINFLUX experiment can come from 1) an imperfect zero in the excitation PSF or 2) auto-fluorescence of the sample or optics or out-of-focus signal from other fluorophores.

Let's consider the behavior of background at $x_0 = 0$. In the case of an imperfect zero, all photons come from the photon budget of the target fluorophore, N_s . Thus, we substitute $N = N_s$, the number of signal photons, in Eq. 28 to get

$$\sigma_{x_0}(x_0 = 0) = \frac{1}{4L\sqrt{N_s}} \sqrt{(L^2 + 8b\sigma_q^2)(L^2 + 12b\sigma_q^2)}. \quad (31)$$

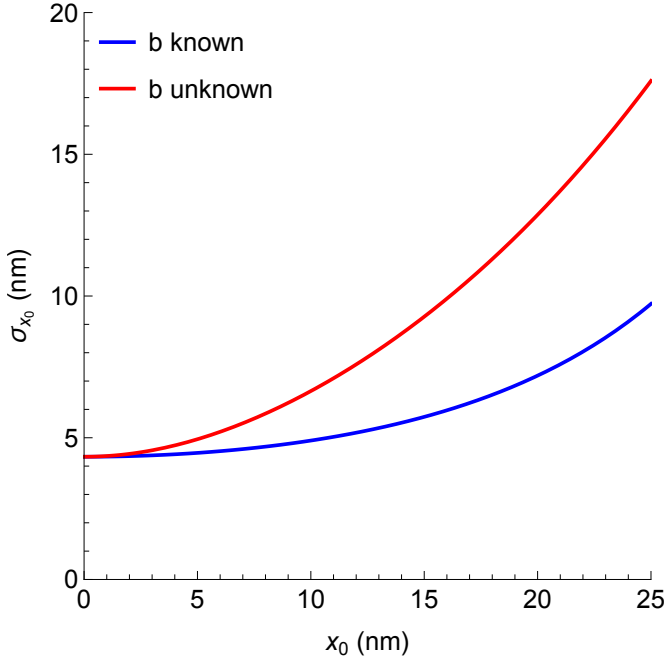


Figure 1: Comparison of the localization precision of an emitter probed at three points with a quadratic minimum in the cases of assumed unknown (Eq. 30) and known (Eq. 27) background, evaluated over emitter position x_0 for $L = 50$ nm, $\sigma_q = 250$ nm, $b = 0.01$ and $N = 100$ photons.

In the case of auto-fluorescence or out-of-focus signal, the background photons, N_b , do not originate from the target fluorophore. We substitute $N = N_s + N_b$ into Eq. 28. We then make the observation that for the $K = 3$ case, when we know the background, $N_b = 3bN_s / (I(-L/2) + I(0) + I(L/2))$. In this case,

$$b_{x_0=0} = \frac{L^2 N_b}{12 N_s \sigma_q^2}. \quad (32)$$

Subsequently, plugging this in to our $N = N_s + N_b$ -substituted version of Eq. 28 we get

$$\sigma_{x_0}(x_0 = 0) = \frac{1}{4\sqrt{N_s}} \sqrt{L^2 + 8b\sigma_q^2}, \quad (33)$$

in the case we have autofluorescence or out-of-focus background. We plot a comparison of this and the imperfect zero case in Figure 2. There is a general trend that as L decreases, the localization precision improves, as expected. However, in the case of background arising from an imperfect zero, too small of an L is dominated by background. We can also see that shrinking $L \rightarrow 0$ does not result in perfect localization precision in the case of autofluorescence or out-of-focus background, and there is a minimum uncertainty generated by the background.

2.2 Maximum

Next, we look at 1D localization with a maximum, corresponding to using confocal-style microscopes. The diffraction-limited, excitation, Airy-function-shaped PSF can be approximated closely by a Gaussian function:

$$I(x_0 - x_i)_{\text{Gauss,1D}} = I_0 \left(e^{-\frac{(x_0 - x_i)^2}{2\sigma_q^2}} + b \right), \quad (34)$$

where I_0 , x_i , x_0 , and b are as defined in Eq. 1 and, as in Eq. 22, the diffraction limit sets a lower bound on the steepness of the PSF, σ_q .

For $b = 0$, the localization precision of a simple single-point measurement with a Gaussian maximum (Eq. 3) is

$$\delta x_0 = \frac{\sigma_q^2}{x_0 \sqrt{N}}. \quad (35)$$

We can use this simple estimate to get an intuition for how a maximum (Eq. 34) will perform as compared to a minimum (Eq. 22). We can see in Figure 3 that the precision in the minimum case (Eq. 23) approaches 0 for $x_0 = 0$, while the precision for the maximum (Eq. 35) improves as it moves further from the emitter position. This tells us 1) the minimum is more sensitive to position than the maximum in the standard measurement range $L < \sigma_q$ and 2) an emitter can be probed at a shorter distance with a minimum excitation PSF, reducing sparsity requirements.

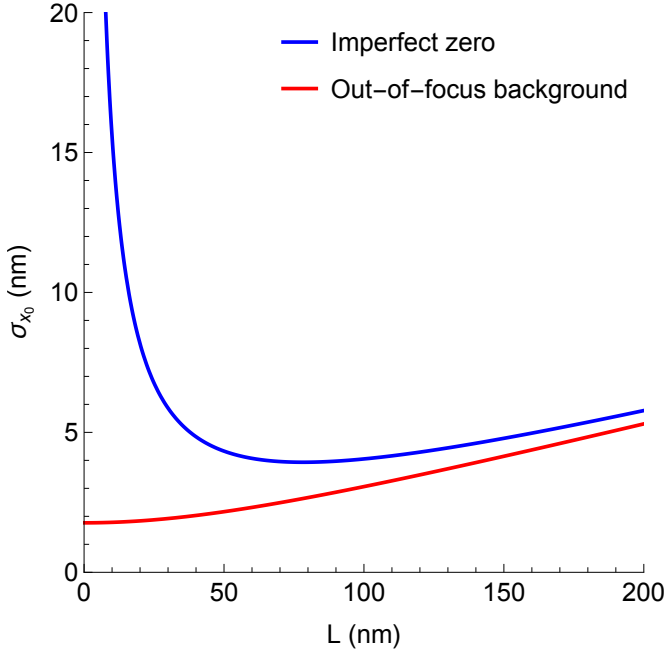


Figure 2: Comparison of σ_{x_0} vs. L at $x_0 = 0$ for an emitter probed with a quadratic minimum at three points and background coming from either an imperfect zero (Eq. 31) or from autofluorescence or out-of-focus emitters (Eq. 33). Here, $b = 0.01$, $\sigma_q = 250$ nm and $N_s = 100$.

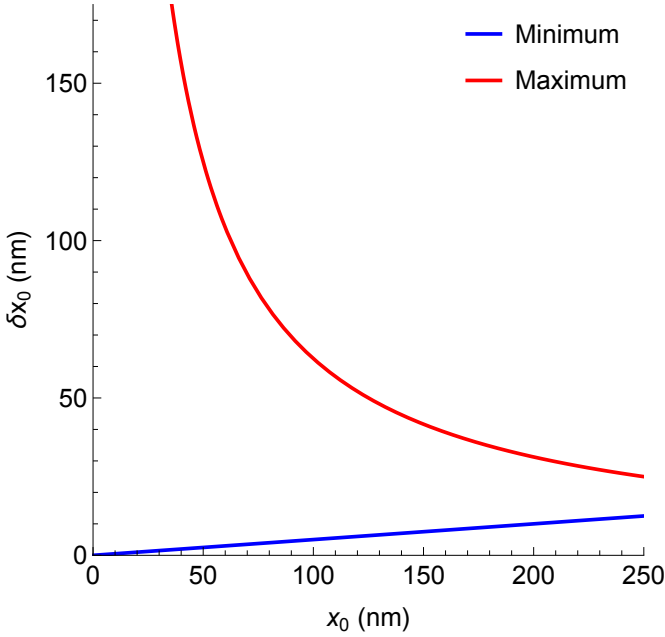


Figure 3: Comparison of first-order emitter localization precision (Eq. 3) arising from minimum (Eq. 22) and maximum (Eq. 34) excitation PSFs evaluated at $\sigma_q = 250$ nm, $N = 100$, and $x_0 = 0$ over a field of view of length σ_q .

2.2.1 Maximum with a known background

Suppose we again measure at two points, $x_i = -L/2$ and $L/2$. When the separation distance $L < \sigma_q$, the maximum of the Gaussian can be approximated as a quadratic equation,

$$I_{\text{negquad,1D}}(x_0 - x_i) = I_0 \left(1 - \frac{(x_0 - x_i)^2}{2\sigma_q^2} + b \right), \quad (36)$$

and so

$$\sigma_{x_0} = \frac{1}{4L\sqrt{N}} \sqrt{\frac{(-8(b+1)\sigma_q^2 + L^2 + 4x_0^2)^2 \left(-16(b+1)(L^2 + 4x_0^2)\sigma_q^2 + 64(b+1)^2\sigma_q^4 + (L^2 - 4x_0^2)^2 \right)}{(-8(b+1)\sigma_q^2 + L^2 - 4x_0^2)^2}}. \quad (37)$$

This has worse localization precision than the corresponding minimum when $L < \sigma_q$, as shown in Figure 4. At

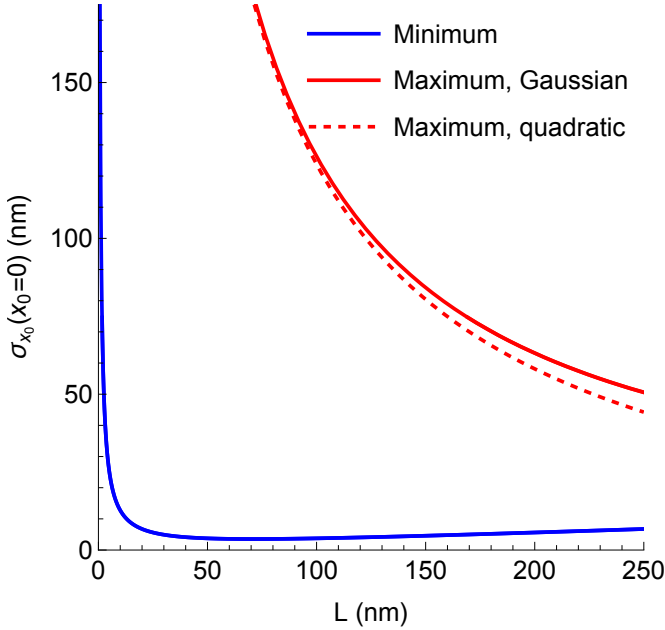


Figure 4: Comparison of localization precision of maximum and minimum probing of an emitter with two point measurements in 1D and with known background. The plot shows σ_{x_0} from Eqs. 39 (maximum, Gaussian), 37 (maximum, quadratic) and 24 (minimum) evaluated at $x_0 = 0$ vs. separation distance L for $\sigma_q = 250$ nm, $b = 0.01$, and $N = 100$ photons. Note that for the optimal choice of L , $L \ll \sigma_q$, the minimum outperforms the maximum.

$x_0 = 0$ and with no background ($b = 0$), Eq. 37 simplifies to

$$\sigma_{x_0}(x_0 = 0, b = 0) = \frac{1}{4L\sqrt{N}} |L^2 - 8\sigma_q^2|. \quad (38)$$

In the range of $L < \sigma_q$, the illumination profile will be near its peak and N will be much higher than in the case of equivalent probing with a minimum. That is, for a fixed L , when $L < \sigma_q$, the emitter will experience a much greater intensity in the maximum case and emit more photons, resulting in a poorer photon efficiency than in the minimum case.

For $L > \sigma_q$, it may be possible to illuminate the emitter with the less intense parts of two Gaussians. In this case, the quadratic approximation does not apply. Using the Gaussian PSF (Eq. 34), we obtain a lengthy expression, which for $x_0 = 0$ simplifies to

$$\sigma_{x_0}(x_0 = 0) = \frac{\sigma_q}{\sqrt{N}} \frac{2\sigma_q}{L} \left(be^{\frac{L^2}{8\sigma_q^2}} + 1 \right). \quad (39)$$

We can see in Figure 4 that the position uncertainty of the Gaussian maximum initially decreases with increasing displacement L . However, as shown in Figure 5, the gradient and magnitude of the Gaussian tails eventually diminish to a point where, in the presence of background, the localization precision gets worse again. This is influenced by the Gaussian width σ_q , which is fundamentally limited by diffraction, and by the strength of the background. We can see in Figure 4 that for the optimal choice of L , $L \ll \sigma_q$, the minimum outperforms the maximum.

For the no background case, the Gaussian PSF CRB simplifies to

$$\sigma_{x_0}(b = 0) = \frac{\sigma_q}{\sqrt{N}} \frac{2\sigma_q}{L} \cosh\left(\frac{Lx_0}{2\sigma_q^2}\right), \quad (40)$$

which is equivalent to the corresponding Eq. S23b in the supplement of [1] in the event that the definition of the Gaussians are made to be in agreement; this means exchanging $\frac{4\log(2)}{fwhm^2}$ in Eq. S19 of the supplement of [1] for $\frac{1}{2\sigma_q^2}$ to match our Eq. 34 (change from calculating via the full width at half maximum to the standard deviation).

Without background ($b = 0$), Eq. 39 simplifies to

$$\sigma_{x_0}(x_0 = 0, b = 0) = \frac{2\sigma_q^2}{L\sqrt{N}}, \quad (41)$$

which is equivalent to the corresponding Eq. S24b in the supplement of [1] and equivalent to Eq. 35 evaluated at $x_0 = L/2$.

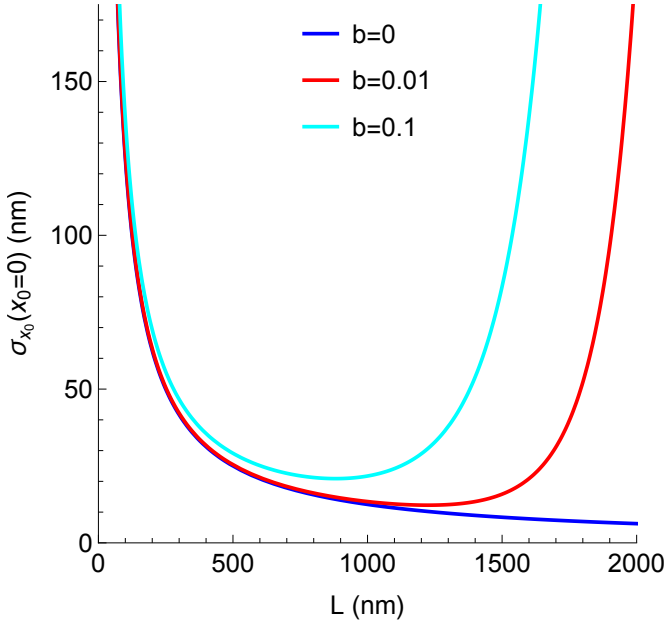


Figure 5: Localization precision for probing an emitter at two points with a Gaussian maximum. The plot shows σ_{x_0} from Eq. 39 vs. separation distance L for $x_0 = 0$, $\sigma_q = 250$ nm and $N = 100$ photons at 3 different background levels.

3 Localization precision of emitters in 2D

The CRB in 2D is almost identical to what was derived in Section 1, but we now swap y_0 for b in the Fisher information matrix. We also now compute the average localization precision, $\sigma_{\text{CRB}} = \sqrt{\frac{1}{2}\text{Tr}(\Sigma_{\text{CRB}})}$, to examine the contributions along both the x and y directions. We will leave b in the definition of $I(x_0 - x_i, y_0 - y_i)$ as a known constant.

3.1 2D MINFLUX with explicit, known background

We want to show that our notation is equivalent to published results [1–3] in 2D as well as 1D. 2D MINFLUX localization precision is often calculated for four measurements of an emitter at $(x_i, y_i) = (0, 0), (-\frac{L}{4}, \frac{\sqrt{3}L}{4}), (-\frac{L}{4}, -\frac{\sqrt{3}L}{4}), (\frac{L}{2}, 0)$ using a donut,

$$I_{\text{donut}}(x_0 - x_i, y_0 - y_i) = I_0 \left(e^{\frac{(x_0 - x_i)^2 + (y_0 - y_i)^2}{2\sigma_q^2}} \exp\left(-\frac{(x_0 - x_i)^2 + (y_0 - y_i)^2}{2\sigma_q^2}\right) + b \right), \quad (42)$$

where I_0 and b are as defined in Eq. 1, the diffraction limit sets a lower bound on the steepness of the PSF, σ_q , (x_0, y_0) is the position of the emitter and (x_i, y_i) is the position of the excitation PSF. Computing the CRB for Eq. 42 at these points and evaluating it at $(x_0, y_0) = (0, 0)$ yields

$$\sigma_{x_0}(x_0 = 0, y_0 = 0) = \frac{\sigma_q}{\sqrt{N}} \frac{\sqrt{8}\sigma_q}{L} \sqrt{\frac{L^2 \left(eL^2 + 8b \exp\left(\frac{L^2}{8\sigma_q^2}\right) \sigma_q^2 \right) \left(3eL^2 + 32b \exp\left(\frac{L^2}{8\sigma_q^2}\right) \sigma_q^2 \right)}{3e^2(L^3 - 8L\sigma_q^2)^2}}. \quad (43)$$

In [1–3], there is no background term in the definition of the donut (Eq. 42). Substituting $b = (I_{\text{donut}}(x_0, y_0) + I_{\text{donut}}(x_0 + \frac{L}{4}, y_0 - \frac{\sqrt{3}L}{4}) + I_{\text{donut}}(x_0 + \frac{L}{4}, y_0 + \frac{\sqrt{3}L}{4}) + I_{\text{donut}}(x_0 - \frac{L}{2}, y_0)) / (4I_0 \text{SBR}(x_0))$, using the definition of SBR (Eq. 11), yields

$$\sigma_{x_0}(x_0 = 0, y_0 = 0) = \frac{\sigma_q}{\sqrt{N}} \frac{\sqrt{8}\sigma_q}{L} \frac{L^2}{8\sigma_q^2 - L^2} \sqrt{\left(\frac{1}{\text{SBR}(x_0)} + 1\right) \left(\frac{3}{4\text{SBR}(x_0)} + 1\right)} \quad (44)$$

If, as for Eq. 40, we assume a Gaussian full width at half maximum, we can make the substitution $\frac{1}{2\sigma_q^2} = \frac{4 \log(2)}{fwhm^2}$. With this substitution, Eq. 44 is equivalent to Eq. S31 in the supplement of [1]. Evaluating Eq. 43 at $b = 0$ yields

$$\sigma_{x_0}(x_0 = 0, y_0 = 0) = \frac{\sigma_q}{\sqrt{N}} \frac{\sqrt{8}\sigma_q}{L} \frac{L^2}{(8\sigma_q^2 - L^2)}, \quad (45)$$

which is equivalent to its corresponding equation S27 in the supplement of [1], again in the case we set $\frac{1}{2\sigma_q^2} = \frac{4 \log(2)}{fwhm^2}$.

3.2 Orbital tracking

In 2D MINFLUX, we measure about an emitter with a donut-shaped minimum. In orbital tracking, instead a Gaussian PSF is used [4]. In fluorophore tracking, we expect the emitter to move and update our orbit about the emitter to be centered on its new position (x_i, y_i) at each time point i . For ease of derivation, we will consider here the case where the excitation PSF orbits a stationary emitter. In this case, the 2D Gaussian PSF is expressed as

$$I_{\text{Gauss,2D}}(x_0 - x_i, y_0 - y_i) = I_0 \left(\exp \left(-\frac{(x_0 - x_i)^2 + (y_0 - y_i)^2}{2\sigma_q^2} \right) + b \right), \quad (46)$$

where I_0 , is the amplitude of the illumination, (x_i, y_i) is the coordinate of the excitation PSF, (x_0, y_0) is the coordinate of the emitter, σ_q parameterizes the steepness of the PSF, and b is the proportion of signal arising from the background.

For most orbital tracing, the movement is continuous and the number of measurements K is large. For ease of computation, let us consider three (or four, or six, or twelve) points evenly spaced on a circle with radius $L/2$, centered on the emitter location (x_0, y_0) . Following the framework established in Section 1, using y_0 instead of b in the Fisher information matrix, and setting $(x_0, y_0) = (0, 0)$, we get

$$\sigma_{x_0, y_0}(x_0 = 0, y_0 = 0) = \frac{\sigma_q}{\sqrt{N}} \frac{\sqrt{8}\sigma_q}{L} \left(b e^{\frac{L^2}{8\sigma_q^2}} + 1 \right). \quad (47)$$

Interestingly, because we achieve the same result for $K = 3, 4, 6$ and 12 , this implies that the CRB at $(x_0, y_0) = (0, 0)$, is independent of the choice of K when σ_q is the same along x and y .

Without background, Eq. 47 suggests that the localization precision can be improved by letting $L \rightarrow \infty$. However, any background leads to a deterioration of the localization precision with large L (Figure 6), leading to an optimal value of $L \approx 5\sigma_q$ [3, 4]. This phenomenon is shown in Figure 6 and is in agreement with the behavior of the two Gaussian measurement in the 1D case (Eq. 39).

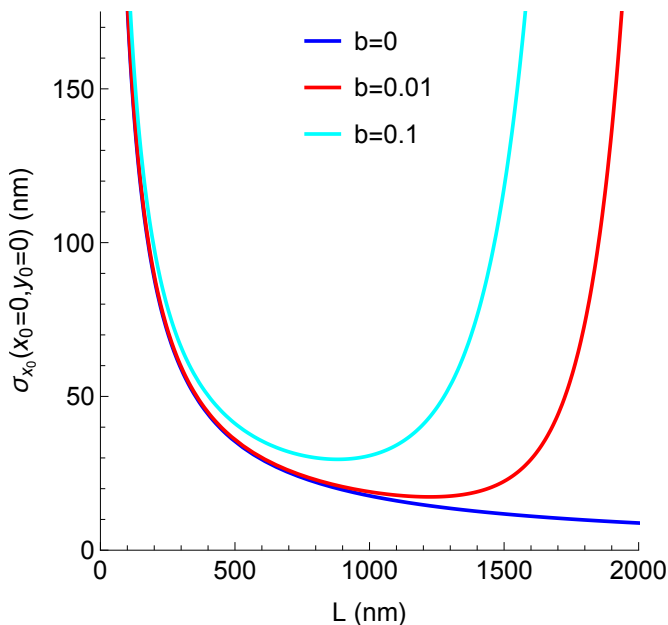


Figure 6: Localization precision for probing an emitter with an orbital tracking scheme. The plot shows σ_{x_0} from Eq. 47 vs. separation distance L for $x_0 = 0$, $\sigma_q = 250$ nm, and $N = 100$ photons at 3 different background levels.

Conclusion

In this paper, we proposed an alternative formulation to the standard signal-to-background approach for background in MINFLUX measurements that allows us to investigate the influence of unknown background on localization precision. We found that this formulation agrees with previous work when the background is known.

Acknowledgements

The authors thank Dr. Sheng Liu, Nikolay Sergeev, Dr. Takahiro Deguchi, Dr. Lukas Scheiderer, and Dr. Francesco Reina for helpful discussions.

References

1. Balzarotti, F. *et al.* Nanometer resolution imaging and tracking of fluorescent molecules with minimal photon fluxes. en. *Science* **355**, 606–612. ISSN: 0036-8075, 1095-9203. <https://www.science.org/doi/10.1126/science.aak9913> (Feb. 2017).
2. Eilers, Y., Ta, H., Gwosch, K. C., Balzarotti, F. & Hell, S. W. MINFLUX monitors rapid molecular jumps with superior spatiotemporal resolution. en. *Proceedings of the National Academy of Sciences* **115**, 6117–6122. ISSN: 0027-8424, 1091-6490. <https://pnas.org/doi/full/10.1073/pnas.1801672115> (June 2018).
3. Masullo, L. A., Lopez, L. F. & Stefani, F. D. A common framework for single-molecule localization using sequential structured illumination. en. *Biophysical Reports* **2**, 100036. ISSN: 26670747. <https://linkinghub.elsevier.com/retrieve/pii/S2667074721000367> (Mar. 2022).
4. Enderlein, J. Tracking of fluorescent molecules diffusing within membranes. en. *Applied Physics B* **71**, 773–777. ISSN: 0946-2171, 1432-0649. <http://link.springer.com/10.1007/s003400000409> (Nov. 2000).